ATOMIC PHYSICS

Seconds-scale coherence on an optical clock transition in a tweezer array

Matthew A. Norcia, Aaron W. Young, William J. Eckner, Eric Oelker, Jun Ye, Adam M. Kaufman*

Coherent control of high–quality factor optical transitions in atoms has revolutionized precision frequency metrology. Leading optical atomic clocks rely on the interrogation of such transitions in either single ions or ensembles of neutral atoms to stabilize a laser frequency at high precision and accuracy. We demonstrate a platform that combines the key strengths of these two approaches, based on arrays of individual strontium atoms held within optical tweezers. We report coherence times of 3.4 seconds, single-ensemble duty cycles up to 96% through repeated interrogation, and frequency stability of 4.7×10^{-16} $(\tau/\mathrm{s})^{-1/2}$. These results establish optical tweezer arrays as a powerful tool for coherent control of optical transitions for metrology and quantum information science.

Optical clocks based on neutral atoms and ions achieve exceptional precision and accuracy (*1*–*6*), with applications in relativistic geodesy (*7*), tests of relativity (*8*), and searches for dark matter (*9*). Achieving such performance requires balancing competing desirable features, including a high particle number, isolation of atoms from collisions, insensitivity to motional effects, and high–duty cycle operation (*10*, *11*).

The leading platforms for optical clocks—based on trapped single ions and ensembles of neutral atoms confined within optical lattices—take distinct approaches in the pursuit of precision and accuracy. Clocks based on single ions use single-particle control and detection to enable high–duty cycle interrogation of an isolated atom (*6*, *12*). Optical lattice clocks, on the other hand, typically interrogate thousands of atoms in parallel to reach exceptionally low atom shot noise, enabling frequency measurements with precision below the part-per-10^{18} level within 1 hour (*2*).

Working with large atom numbers creates challenges associated with laser frequency noise aliasing and interatomic collisions, which can be difficult to address simultaneously. Frequency noise aliasing through the so-called Dick effect arises from dead time between subsequent interrogations of the atoms (*13*). Methods have been developed to overcome dead-time effects by interleaving interrogation of two independent clock ensembles in separate chambers (*2*, *14*), and techniques for high-precision nondestructive detection have been explored (*15*, *16*).

Interatomic collisions can limit both the precision and accuracy of a clock, but they can be mitigated by isolating the atoms from one another. This has recently been demonstrated in a Fermi-degenerate optical lattice clock, in which a well-defined number of atoms occupies each lattice site (*17*). This approach relies on evaporative cooling and a quantum phase transition in the Hubbard model ground state, and therefore typically requires long gaps between clock interrogations, leading to increased sensitivity to noise aliasing. The sub–micrometer-scale optical lattices essential for such Hubbard-regime physics also limit the current record for atom-light coherence (8 s), because dephasing from atomic tunneling must be balanced against decoherence attributable to scattering from the lattice (*17*, *18*). This suggests that the next frontier in atomic coherence will require new tools that allow control of the atomic spacing (*18*).

Here, we demonstrate the core capabilities for an optical-frequency metrology platform based on arrays of individual strontium atoms trapped in optical tweezers (see Fig. 1A). The platform combines the high duty cycle and microscopic control techniques of ion clocks with the scaling capacity inherent in neutral atoms, and it allows for a high degree of atomic isolation and coherence. The single-atom occupancy readily achieved in tweezers eliminates perturbations associated with atomic collisions; the low temperatures and relatively large spatial separation between tweezers can suppress motional and tunneling effects. The tweezer platform also enables rapid, state-selective, nondestructive detection (*19*–*24*) and thus repeated clock interrogation of the same atoms. These experimental conditions allow the duty cycles, stability, and atom-optical coherence reported in this work.

Combining coherent control of the clock transition with the microscopic control afforded by optical tweezers may also prove useful in several subfields of quantum information science more broadly. Such control is necessary for proposals for quantum gates based on spin-orbital exchange interactions (*25*–*27*). Further, single-photon Rydberg transitions from the excited clock state allow access to many-body spin models and gate architectures with fast time scales relative to dissipation rates, which may lead to improvement over analogous schemes with alkali species (*28*–*30*). Rydberg dressing on the clock transition of microscopically controlled atoms also provides a clear path to the generation of entangled states with improved metrological performance (*31*, *32*), a long-standing goal for optical clocks.

Our platform (*21*) consists of one-dimensional arrays of neutral, bosonic ^{88}Sr atoms that are tightly confined within optical tweezers and cooled using three-dimensional sideband cooling (Fig. 1). With each run of our experiment, individual tweezers have an approximately 50% probability of being empty or of containing a single atom; multiple occupancies are suppressed by light-assisted collisions (*33*). For the current work, we use 10 traps, generated by applying 10 radio-frequency tones to an acousto-optic deflector. Imaging is performed with negligible atom loss by simultaneously scattering photons on the broad $^1S_0$ to $^1P_1$ transition at 461 nm and cooling on the narrow-linewidth $^1S_0$ to $^3P_1$ transition at 689 nm (*21*, *22*, *24*).

We interrogate the $^1S_0$ to $^3P_0$ optical "clock" transition, which is induced in our bosonic atoms by applying a magnetic field (*3*, *34*), using light from a highly stable laser referenced to a crystalline optical cavity (*2*). Magnetic field values of 0.14 to 2.2 mT and probe intensities ranging from 50 mW/cm^2 to 5 W/cm^2 are used to generate Rabi frequencies from 0.125 Hz for our narrowest-linewidth Rabi spectroscopy up to 17 Hz for Ramsey spectroscopy (*35*). By comparing images of the atomic array taken before and after probing, we infer the excitation to the $^3P_0$ state from the apparent loss of atoms in the $^1S_0$ ground state. Because the imaging is highly nondestructive (*23*, *24*), we can repeat this interrogation cycle many times before preparing a new ensemble of atoms (Fig. 1B). The tweezer light has a wavelength near 813.4272 nm, where the light shifts to $^1S_0$ and $^3P_0$ are nearly equal [the so-called "magic wavelength" (*36*)]. The use of a "magic angle" technique (*21*) allows us to also achieve state-insensitive trapping on the $^1S_0$ to $^3P_1$ transition at this wavelength, enabling sideband cooling to average phonon numbers of 0.2 along the axis of the clock interrogation.

These conditions enable coherent atom-light interactions on seconds-long time scales. Figure 1B (inset) shows the inferred excitation probability associated with a 1.5-s laser probe pulse as a function of laser frequency, with the intensity of the probe pulse tuned to maximize transfer probability. The full width at half maximum (FWHM) of this feature is below 500 mHz, extracted by fitting a Gaussian function to the excitation probability. We further characterize the atom-light coherence

JILA, University of Colorado and National Institute of Standards and Technology, and Department of Physics, University of Colorado, Boulder, CO 80309, USA.
*Corresponding author. Email: adam.kaufman@colorado.edu

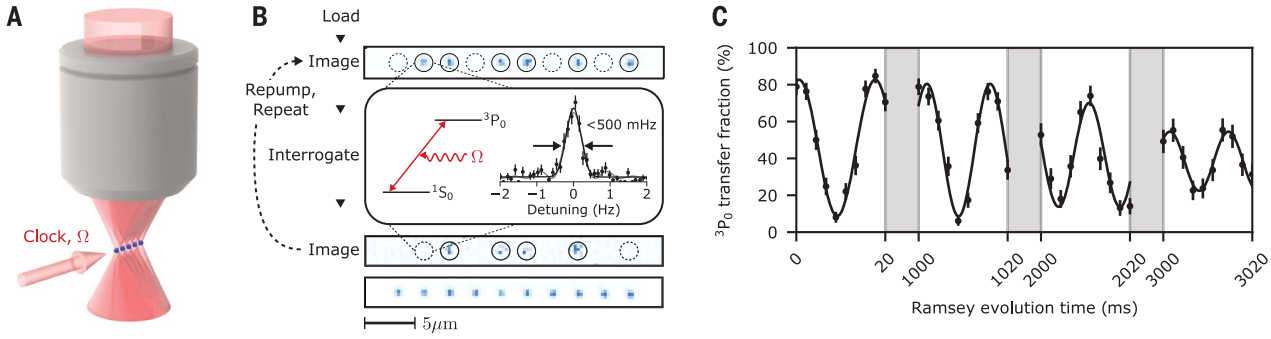

Fig. 1. Clock transition interrogation in an optical tweezer array. (**A**) Apparatus for interrogation of $^1S_0$ to $^3P_0$ "clock" transition in tweezer arrays of strontium atoms. Using a high–numerical aperture (NA > 0.65) objective, we project tightly confining optical potentials to trap single strontium atoms. By tuning these traps near the so-called "magic" wavelength, we can ensure that the clock transition is minimally sensitive to the local intensity experienced by the atoms. (**B**) Repeated interrogation of clock transition. Top: Image of a single ensemble of atoms loaded into tweezers with ~50% filling. After interrogating the clock transition, excitation of the $^3P_0$ state can be inferred from apparent atom loss in a second image. By repumping atoms between interrogation cycles, each ensemble can be interrogated many times before losing atoms. Bottom: Image averaged over many such ensembles. Inset: Narrow-line Rabi spectrum of clock transition retrieved without repeated interrogation. Fits to sinc and Gaussian functions are shown in gray and black, respectively. In this case, a 1.5-s probe yields an approximately Fourier-limited Gaussian linewidth of 450 ± 20 mHz. (**C**) Ramsey spectroscopy in 200-photon recoil energy (E_R) deep tweezers, showing a coherence time of 3.4 ± 0.4 s. The frequency of the fringes is set by the differential light shift imposed on the clock transition by the probe beam. These data were taken using the repeated imaging technique outlined in the text.

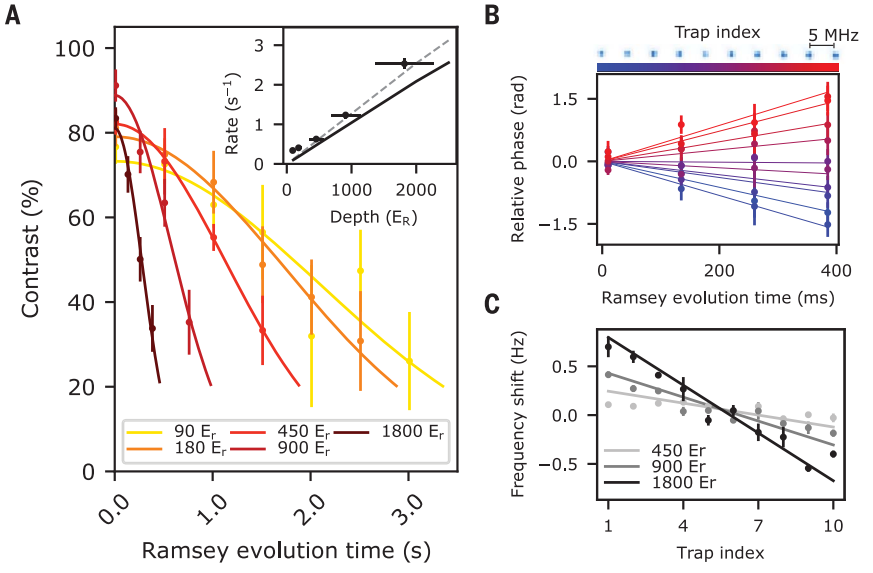

Fig. 2. Single-site resolved coherence studies. (**A**) Ramsey contrast as a function of evolution time for different trap depths, showing tweezer-induced contrast decay. Inset: 1/*e* Gaussian decay rates for Ramsey contrast versus tweezer depth, in units of the tweezer photon recoil energy E_R. For deep tweezers, contrast decay rate is proportional to tweezer depth. This can largely be explained by variations in the frequency of the trapping light across the tweezer array as a result of different radio-frequency tones used to generate the tweezer spots, whose expected contribution is represented by the black line. The combined expectation of both this effect and Raman scattering, as inferred from measured depopulation rates from $^3P_0$, is illustrated by the gray dashed line (*18*, *35*). (**B**) Measured relative Ramsey phase shifts for individual traps in 1800-E_R tweezers. (**C**) Inferred relative frequency shifts for individual tweezers at different depths, with predictions based on the known sensitivity to trap detuning (*37*, *38*).

through Ramsey spectroscopy, where we scan the duration of the gap between two π/2 pulses from the clock laser. Because the laser is held at the probe light–shifted resonance frequency of the clock transition, we observe oscillations in the final transfer fraction occurring at the difference between this frequency and that of the bare clock transition. The contrast of these oscillations persists with a 1/*e* decay time of up to 3.4 ± 0.4 s (Fig. 1C), providing a measure of our atom-light coherence and a bound on our atom-atom coherence.

We observe more rapid decay of Ramsey contrast when operating with deep tweezers, with a rate that depends linearly on the depth of the tweezers (Fig. 2A). This can be largely attributed to slight variations in the optical frequencies of the tweezer light across the different traps, stemming from the different radio-frequency tones applied to the acousto-optic deflector (adjacent tweezers are separated by 5 MHz). Because of this frequency difference, all traps cannot be operated at exactly the magic wavelength at the same time. The predicted magnitude of this effect is illustrated by the black line in the inset of Fig. 2A; the dashed gray line is an expectation that shows the combined effect of this non-magic behavior and the Raman scattering from the excited state (*18*). We use the spatial resolution of our system to study this dephasing effect at a single-atom level in Fig. 2, B and C. For the deepest tweezers used in Fig. 2A, we fit the phase of the Ramsey fringes for each site in the array at different hold times. We observe a relative shift in this phase between tweezers that increases linearly with hold time and with the distance from the center of the array (Fig. 2B), from which we extract the relative frequency shifts between atoms in different tweezers. These frequency shifts are plotted in Fig. 2C for selected depths, and they agree well with predictions based on the known derivative of the differential polarizability of the clock transition, −15.5 ± 1.1 (μHz/E_R)/MHz (*37*, *38*). To eliminate this dephasing mechanism in the future, the tweezers could be projected using a digital

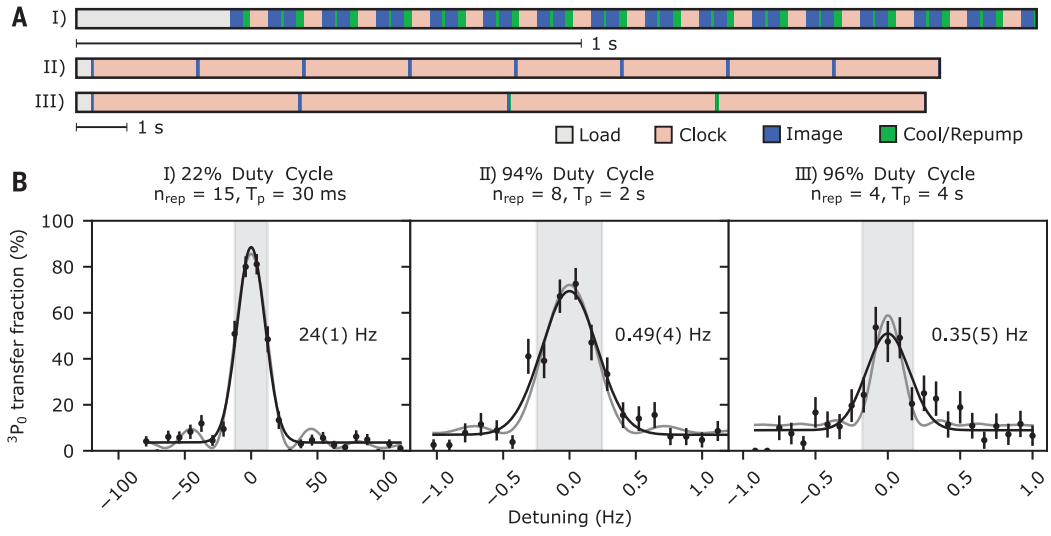

Fig. 3. Repeated nondestructive interrogation of the clock transition. (**A**) Timing diagram for repeated interrogation of the clock transition for various clock interrogation times (T_p) and number of repeated interrogations (n_{rep}): (I) n_{rep} = 15, T_p = 30 ms; (II) n_{rep} = 8, T_p = 2 s; (III) n_{rep} = 4, T_p = 4 s. These repetition numbers are chosen on the basis of experimental convenience: High repetition numbers have a more substantial impact on duty cycle for short interrogation times, but owing to stochastic loading, they require lengthy data scans for long probe times to achieve uniform statistical uncertainty. (**B**) Corresponding Rabi spectra for sequences I to III. Sinc fits are shown in gray, Gaussian fits in black. Shaded regions and labels correspond to Gaussian FWHM.

mirror device or spatial light modulator, for which all traps have the same optical frequency.

For trap depths below 200 times the photon recoil energy E_R associated with the tweezer light, we find that the improvements in coherence time begin to saturate, indicating the presence of other decoherence mechanisms such as residual path-length fluctuations between the clock laser and the atoms. Further, we find that the initial contrast of oscillations decreases in shallow tweezers, which could be due to residual atomic motion. All spectroscopic measurements presented in this work were performed in tweezers with depths of 200 E_R unless otherwise stated.

The alkaline-earth tweezer platform enables nondestructive, state-selective imaging (*23*, *24*), which we can use to interrogate the same ensemble of atoms many times and realize high–duty cycle interrogation of the clock transition. This both improves the rate at which statistical uncertainty can be averaged down and mitigates noise aliasing of the clock laser (*35*). Each interrogation cycle involves 90 ms of dead time during which the clock transition is not being interrogated, compared to approximately 300 ms to load new atoms into the tweezers (Fig. 3). For short (30 ms) interrogation pulses, we observe a loss probability of 0.001 (±0.001) per cycle. For longer cycle times (up to 8 s), we observe a total loss probability consistent with 0.01 per second for atoms prepared in either the ground or excited state, likely caused by collisions with the background gas.

The coherence properties of clock interrogation with repeated imaging are consistent with those when each set of atoms is interrogated only once. Ramsey contrast curves with coherence times of 3 s have been measured using both repeated and single interrogation, as shown in Figs. 1C and 2A, respectively. Figure 3 characterizes this repeated interrogation technique for different clock probe durations (T_p) and numbers of cycles (n_{rep}) performed using the same ensemble of atoms. In Fig. 3B, we use interrogation pulse durations up to 4 s to demonstrate duty cycles as high as 96% and clock spectra as narrow as 350 mHz.

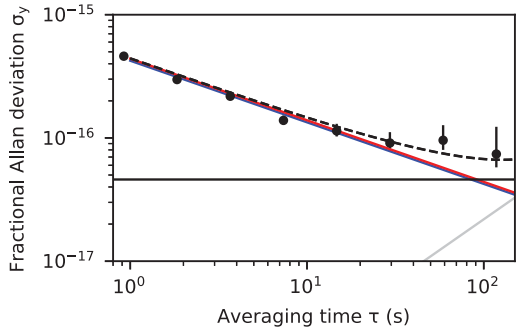

Fig. 4. Characterization of frequency stability. The short-term stability of the atomic clock signal relative to the interrogation laser is quantified in terms of the Allan deviation of fractional frequency fluctuations. For Ramsey interrogation with 500 ms between pulses, we fit a fractional instability of $4.7 \times 10^{-16}\ (\tau/s)^{-1/2}$ at short averaging times (red line), consistent with the expected atom shot noise limit after accounting for our measured contrast (blue line). The flicker noise and known drift of the laser are represented by the black and gray traces, respectively, and the predicted combination of atom shot noise, laser noise, and laser drift by the dashed line.

We characterize the short-term stability of the atomic frequency reference by computing the Allan deviation relative to the free-running clock laser (Fig. 4). This measurement is performed using single-interrogation (n_{rep} = 1) Ramsey spectroscopy with evolution times of 501 ms, chosen to bias the signal to the most sensitive part of the Ramsey fringe. The clock laser was not actively stabilized to the atomic transition, which limits the total length of the dataset to 500 s. Under these conditions, we measure a fractional frequency instability of $4.7 \times 10^{-16}\ (\tau/s)^{-1/2}$ at short times. As expected, this is dominated by the atomic quantum projection noise associated with the average atom number of 4.8 per trial, whereas the long-term instability is consistent with known drifts in the frequency of our laser (*35*).

Currently, our demonstrated instability falls between that attained with single ions (*6*) and in optical lattice clocks operating with thousands of atoms (*1*–*4*). Achieving stability competitive with the most stable optical lattice clocks [$4.8 \times 10^{-17}\ (\tau/s)^{-1/2}$ (*2*)] could be achieved with increased atom number—for example, by using a dark time of 2 s and approximately 150 atoms. Because of our high duty cycle and low-noise laser system, Dick effect noise would contribute only modestly (16% and 6% of noise variance for individual and 16 times–repeated interrogation, respectively). Although we demonstrate coherence times exceeding 2 s in this

work, attaining this atom number would require more power than is available with our current system (here, we use 13 ± 1 mW per tweezer spot into the objective for cooling and imaging). However, by performing atomic preparation and imaging in tweezers at a wavelength with higher polarizability, smaller spot size, and higher available power (such as 515 nm) and then transferring into 813-nm tweezers for clock interrogation, ensemble sizes of 500 atoms or larger could plausibly be achieved, which would enable stability exceeding the current state of the art.

In addition to enabling one to take full advantage of the reduced projection noise associated with large numbers of atoms, the low dead times provided by our tweezer platform would allow one to achieve high performance with a less stable clock laser. This capability could be especially transformative for high-performance portable optical clocks (*7*), where technical constraints limit the performance of the clock laser (*39*). In this context, our repeated imaging technique would allow for relatively high duty cycles even with short interrogation times, thereby greatly improving the stability associated with both quantum projection noise and laser noise aliasing (*35*).

For use as an absolute frequency reference, systematic shifts to the clock transition frequency must be carefully considered. Many of the shifts present in the tweezer platform, particularly environmental perturbations such as blackbody radiation, are identical to those present in optical lattice clocks and have been studied in detail (*10*, *11*). In this work, we use bosonic ^{88}Sr atoms. Although this choice is not fundamental to our tweezer platform, it does require consideration of different systematic effects from the more commonly used fermions. Shifts caused by atomic collisions are of particular concern in clocks operating with bosonic atoms (*3*) but are mitigated in the tweezer platform by single-atom occupancy. The use of the bosonic isotope requires higher probe intensities and a relatively large applied magnetic field to reach a given Rabi frequency, so second-order Zeeman and probe-induced Stark shifts can be important. For narrowline Rabi spectroscopy, our probe intensities and magnetic fields are similar to those of (*3*), where their contributions to clock inaccuracy were bounded to the 10^{-17} level. Unlike conventional optical lattices, tweezer confinement relies on tightly focused beams that can have nonuniform polarization at the location of the atoms. Such inhomogeneous polarization could complicate magic trapping in fermionic isotopes, but its effect is expected to be suppressed in bosons, whose clock states have zero net angular momentum (*40*). Finally, in our current setup there are several meters of optical path between the atoms and the surface to which the phase of the interrogation laser is referenced. Fluctuations in this path length lead to Doppler shifts, which can limit stability and, in principle, accuracy. In analogy to techniques used in optical lattice clocks, this could be addressed by referencing the phase of the interrogation laser to a surface rigidly connected to the microscope objective, as this primarily defines the atoms' locations. Characterization of these potential systematic effects associated with the tweezer platform, as well as those unforeseen, will be critical to future studies of clock accuracy.

The ability to control and measure the positions and states of individual atoms may enable opportunities both for extending single-atom coherence and for using ensembles of many atoms in previously unexplored ways. At a single-particle level, the spatial control afforded by the tweezers could allow one to simultaneously suppress tunneling and light-induced decoherence to push coherence times beyond 10 s (*18*). When using many atoms, the microscopic control afforded by the tweezers, combined with interactions introduced using Rydberg dressing (*31*, *32*), could facilitate the creation of entangled states that can surpass the limitations set by atomic projection noise, for fundamental studies of entanglement on an optical clock transition as well as quantum-enhanced high-bandwidth sensors. Future extensions of the imaging and coherent manipulation techniques demonstrated here, in which sub-ensembles of the atoms are manipulated independently, could also allow for techniques that extend interrogation time beyond the coherence time of the laser (*14*) in systems using a single vacuum chamber.

Note added in proof: During review of this manuscript, we became aware of related work (*41*).

REFERENCES AND NOTES

1. W. F. McGrew *et al.*, *Nature* **564**, 87–90 (2018).
2. E. Oelker *et al.*, *Nat. Photonics* 10.1038/s41566-019-0493-4 (2019).
3. S. Origlia *et al.*, *Phys. Rev. A* **98**, 053443 (2018).
4. I. Ushijima, M. Takamoto, M. Das, T. Ohkubo, H. Katori, *Nat. Photonics* **9**, 185–189 (2015).
5. B. J. Bloom *et al.*, *Nature* **506**, 71–75 (2014).
6. C. W. Chou, D. B. Hume, J. C. J. Koelemeij, D. J. Wineland, T. Rosenband, *Phys. Rev. Lett.* **104**, 070802 (2010).
7. J. Grotti *et al.*, *Nat. Phys.* **14**, 437–441 (2018).
8. C. W. Chou, D. B. Hume, T. Rosenband, D. J. Wineland, *Science* **329**, 1630–1633 (2010).
9. A. Arvanitaki, J. Huang, K. Van Tilburg, *Phys. Rev. D* **91**, 015015 (2015).
10. A. D. Ludlow, M. M. Boyd, J. Ye, E. Peik, P. O. Schmidt, *Rev. Mod. Phys.* **87**, 637–701 (2015).
11. N. Poli, C. W. Oates, P. Gill, G. M. Tino, *Riv. Nuovo Cim.* **36**, 555–624 (2013).
12. P. O. Schmidt *et al.*, *Science* **309**, 749–752 (2005).
13. G. Dick, in *Proceedings of the 34th Annual Precise Time and Time Interval Systems and Applications Meeting* (ION, 1987), pp. 133–147; https://tycho.usno.navy.mil/ptti/1987papers/Vol%2019_13.pdf.
14. M. Schioppo *et al.*, *Nat. Photonics* **11**, 48–52 (2017).
15. G. Vallet *et al.*, *New J. Phys.* **19**, 083002 (2017).
16. M. A. Norcia, J. K. Thompson, *Phys. Rev. A* **93**, 023804 (2016).
17. S. L. Campbell *et al.*, *Science* **358**, 90–94 (2017).
18. R. B. Hutson, A. Goban, G. E. Marti, J. Ye, arXiv 1903.02498 [physics.atom-ph] (6 March 2019).
19. A. Fuhrmanek, R. Bourgain, Y. R. Sortais, A. Browaeys, *Phys. Rev. Lett.* **106**, 133003 (2011).
20. M. J. Gibbons, C. D. Hamley, C.-Y. Shih, M. S. Chapman, *Phys. Rev. Lett.* **106**, 133002 (2011).
21. M. A. Norcia, A. W. Young, A. M. Kaufman, *Phys. Rev. X* **8**, 041054 (2018).
22. A. Cooper *et al.*, *Phys. Rev. X* **8**, 041055 (2018).
23. S. Saskin, J. T. Wilson, B. Grinkemeyer, J. D. Thompson, *Phys. Rev. Lett.* **122**, 143002 (2019).
24. J. P. Covey, I. S. Madjarov, A. Cooper, M. Endres, *Phys. Rev. Lett.* **122**, 173201 (2019).
25. D. Hayes, P. S. Julienne, I. H. Deutsch, *Phys. Rev. Lett.* **98**, 070501 (2007).
26. A. J. Daley, M. M. Boyd, J. Ye, P. Zoller, *Phys. Rev. Lett.* **101**, 170504 (2008).
27. G. Pagano, F. Scazza, M. Foss-Feig, *Adv. Quantum Technol.* **2**, 1800067 (2019).
28. H. Bernien *et al.*, *Nature* **551**, 579–584 (2017).
29. T. Wilk *et al.*, *Phys. Rev. Lett.* **104**, 010502 (2010).
30. L. Isenhower *et al.*, *Phys. Rev. Lett.* **104**, 010503 (2010).
31. L. I. R. Gil, R. Mukherjee, E. M. Bridge, M. P. A. Jones, T. Pohl, *Phys. Rev. Lett.* **112**, 103601 (2014).
32. R. Kaubruegger *et al.*, arXiv 1908.08343 [quant-ph] (22 August 2019).
33. N. Schlosser, G. Reymond, I. Protsenko, P. Grangier, *Nature* **411**, 1024–1027 (2001).
34. A. V. Taichenachev *et al.*, *Phys. Rev. Lett.* **96**, 083001 (2006).
35. See supplementary materials.
36. J. Ye, H. J. Kimble, H. Katori, *Science* **320**, 1734–1738 (2008).
37. C. Shi *et al.*, *Phys. Rev. A* **92**, 012516 (2015).
38. T. Takano, R. Mizushima, H. Katori, *Appl. Phys. Express* **10**, 072801 (2017).
39. S. Koller *et al.*, *Phys. Rev. Lett.* **118**, 073601 (2017).
40. A. Taichenachev, V. Yudin, C. W. Oates, *Phys. Rev. A* **76**, 023806 (2007).
41. I. S. Madjarov *et al.*, arXiv 1908.05619 [physics.atom-ph] (15 August 2019).
42. M. A. Norcia *et al.*, Data for "Seconds-scale coherence on an optical clock transition in a tweezer array"; doi:10.5281/zenodo.3381664.

ACKNOWLEDGMENTS

We thank T. Bothwell, M. Brown, J. Cline, A. Goban, R. Hutson, B. Johnston, D. Kedar, C. Kennedy, A. Ludlow, W. Milner, C. Regal, J. Robinson, C. Sanner, J. A. Muniz Silva, L. Sonderhouse, J. K. Thompson, and J. Thompson for discussions and support. **Funding:** Supported by ARO, AFOSR, DARPA, the National Science Foundation Physics Frontier Center at JILA (1734006), and NIST. M.A.N. and E.O. acknowledge support from the NRC research associateship program. **Author contributions:** M.A.N., A.W.Y., W.J.E., and A.M.K. designed, constructed, and operated the tweezer platform. E.O. and J.Y. designed, constructed, and operated the stable laser system. All authors contributed to analysis, discussion of results, and preparation of the manuscript. **Competing interests:** The authors have no competing interests to declare. **Data and materials availability:** The data can be accessed at Zenodo (*42*).

SUPPLEMENTARY MATERIALS

science.sciencemag.org/content/366/6461/93/suppl/DC1
Materials and Methods
Supplementary Text
Figs. S1 to S5
Table S1

16 May 2019; accepted 3 September 2019
Published online 12 September 2019
10.1126/science.aay0644

Science

Seconds-scale coherence on an optical clock transition in a tweezer array

Matthew A. Norcia, Aaron W. Young, William J. Eckner, Eric Oelker, Jun Ye and Adam M. Kaufman

Science **366** (6461), 93-97.
DOI: 10.1126/science.aay0644originally published online September 12, 2019

Building up an optical clock

Arrays of optical tweezers can be used to trap atoms, which can then be manipulated individually. Such arrays have shown promise in quantum simulation of many-body systems. Norcia *et al.* now demonstrate that they can also be used as a platform for optical clocks. The researchers lined up 10 optical tweezers in a one-dimensional array, where each tweezer held either one or zero atoms of strontium. The atoms were subjected to laser light whose frequency was tuned to a clock transition in strontium. By monitoring the number of atoms in each tweezer, the researchers measured a long coherence time of a few seconds. Increasing the number of tweezers should improve the figures of merit of this platform.

Science, this issue p. 93